and other metalloisobacteriochlorins should be reassessed.

Finally, it should be noted that the difference in the forms of the vibrational eigenvectors of OEiBC versus OEP (or versus other types of macrocycles) does not imply that the skeletal-mode frequencies of hydroporphyrins are any less sensitive to the structure of the ring than those of porphyrins. Instead, the differences in the eigenvectors suggest that the frequency–structure correlations are different between the ring systems. This is inherently reasonable in view of the substantial structural differences between these various classes of macrocycles.

Acknowledgment. This work was supported by Grant GM-36243 (D.F.B.) from the National Institute of General Medical Sciences.

Photolysis of Covalent Compounds Composed of Stable Anions and Cations. Transient Absorption Studies on Coordination Complexes Formed from the Triphenylcyclopropenyl Cation and Malonitrilo, Acetonitrilo, and Fluorenyl Anions

Norbert J. Pienta,*,† Robert J. Kessler,† Kevin S. Peters,‡ Erin D. O'Driscoll,‡ Edward M. Arnett,§ and Kent E. Molter§

Contribution from the Department of Chemistry, University of North Carolina, Chapel Hill, North Carolina 27599-3290, Department of Chemistry and Biochemistry, University of Colorado, Boulder, Colorado 80309-0215, and Department of Chemistry, Duke University, Durham, North Carolina 27706. *Received February 8, 1990. Revised Manuscript Received January 14, 1991*

Abstract: A series of molecules (1,2,3-triphenylcyclopropene (**1**), [3-(1,2,3-triphenylcyclopropenyl)](4′-cyanophenyl)malonitrile (**2**), [3-(1,2,3-triphenylcyclopropenyl)](4′-nitrophenyl)malonitrile (**3**), [3-(1,2,3-triphenylcyclopropenyl)](3′-nitrophenyl)malonitrile (**4**), [3-(1,2,3-triphenylcyclopropenyl)](4′-nitrophenyl)acetonitrile (**5**), and [3-(1,2,3-triphenylcyclopropenyl)]-9′-cyanofluorene (**6**), each composed of a stable carbanion and carbocation covalently attached to each other, has been photolysed with use of picosecond and nanosecond laser techniques. These molecules undergo a sequence of events that begins with absorption of a photon by one of two localized chromophores in each precursor (i.e., the stilbene of TPCP or the aryl portion of the starting carbanion). The singlet excited states initiate an electron transfer event at rates that were too fast to measure under the conditions employed. (The radical ions were observed within the shortest available time scale, ca. 25 ps.) The radical ion pairs have two possible alternatives: (1) back electron transfer to form the triplet excited state of the triphenylcyclopropenyl part and (2) bond fragmentation of the central bond (i.e., the one connecting the carbanion to the carbocation). Apparently, the presence of ions from the latter fragmentation depends on the relative rates of the two processes.

Radical and ion intermediates play a critical role in mechanistic organic chemistry. In the last few years, one of us has established a research effort that is investigating aspects that control the equilibria among the three states: the pair of cations C^+ and A^-, the pair of radicals $C^\bullet$ and $A^\bullet$, and the covalent complex C–A (Scheme I).[1] As a result, both thermodynamic and kinetic data are available for a variety of complexes that undergo spontaneous heterolysis and homolysis in solution at room temperature. The previous studies have described the behavior of a wide variety of systems at or near their equilibria. Data include the equilibrium constants, enthalpies to form the central bond, and rates of bond fragmentation and coordination. In the present study, a number of these compounds and related ones have been photolyzed in an attempt to access the radicals and ions at a point far from equilibrium with their covalent precursors. Thus, in this paper, data are included for a series of related complexes (C–A, where C and A refer to the cation and anion from which the starting materials are made):[2] 1,2,3-triphenylcyclopropene (**1**), [3-(1,2,3-triphenylcyclopropenyl)](4′-cyanophenyl)malonitrile (**2**), [3-(1,2,3-triphenylcyclopropenyl)](4′-nitrophenyl)malonitrile (**3**), [3-(1,2,3-triphenylcyclopropenyl)](3′-nitrophenyl)malonitrile (**4**), [3-(1,2,3-triphenylcyclopropenyl)](4′-nitrophenyl)acetonitrile (**5**), [3-(1,2,3-triphenylcyclopropenyl)]-9′-cyanofluorene (**6**) (Figure 1).

The use of picosecond laser techniques enables comprehensive studies on the crossing of excited-state potential surfaces with those for homolytic and heterolytic bond cleavage.[3] Analogous nanosecond techniques bridge the time frame between the picosecond experiments (in which we can and do observe excited states and

Scheme I. Equilibria among Coordination Complex, Ion Pair, and Radical Pair

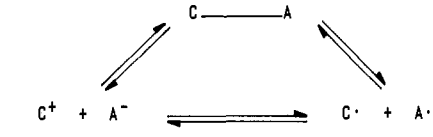

† University of North Carolina.
‡ University of Colorado.
§ Duke University.

(1) (a) Arnett, E. M.; Troughton, E. B. *Tetrahedron Lett.* **1983**, *24*, 3229. (b) Arnett, E. M.; Troughton, E. B.; McPhail, A.; Molter, K. E. *J. Am. Chem. Soc.* **1983**, *105*, 6172. (c) Troughton, E. B.; Molter, K. E.; Arnett, E. M. *Ibid.* **1984**, *106*, 6726. (d) Arnett, E. M.; Chawla, B.; Molter, K. E.; Amarnath, K.; Healy, M. *Ibid.* **1985**, *107*, 5288. (e) Arnett, E. M.; Molter, K. E. *J. Phys. Chem.* **1986**, *90*, 471. (f) Arnett, E. M.; Molter, K. E. *Acc. Chem. Res.* **1985**, *18*, 339. (g) Arnett, E. M.; Molter, K. E.; Marchot, E. C.; Donovan, W. H.; Smith, P. *J. Am. Chem. Soc.* **1987**, *109*, 3788. (h) Arnett, E. M.; Whitesell, L. G., Jr.; Cheng, J.-P.; Marchot, E. C. *Tetrahedron Lett.* **1988**, *29*, 1507. (i) Arnett, E. M.; Amarnath, K.; Harvey, N. G.; Cheng, J.-P. *J. Am. Chem. Soc.* **1990**, *112*, 344.

(2) For the compounds reported herein, C = 1,2,3-triphenylcyclopropenyl, or TPCP for short. The incipient anionic portions A are (4-cyanophenyl)-malonitrilo, CMN; (4-nitrophenyl)malonitrilo, NMN; (3-nitrophenyl)malonitrilo, MET; (4-nitrophenyl)acetonitrilo, NAN; 9-cyanofluorenyl, CFL; and hydrogen, H. Covalent compounds will appear as C–A (e.g., TPCP–CMN), while the intermediates will be drawn as C^+ or $A^\bullet$ (e.g., $TPCP^+$ or $CMN^\bullet$). The term "coordination complex" is the accepted nomenclature for the covalent molecules denoted as C–A (see ref 1).

(3) Peters, K. S. *Ann. Rev. Phys. Chem.* **1987**, *38*, 253–70 and references cited therein.

0002-7863/91/1513-3773$02.50/0

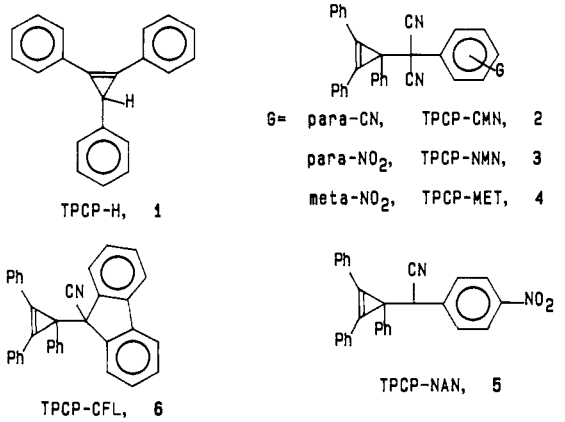

Figure 1. Structures of coordination complexes irradiated. Abbreviations are in ref 2.

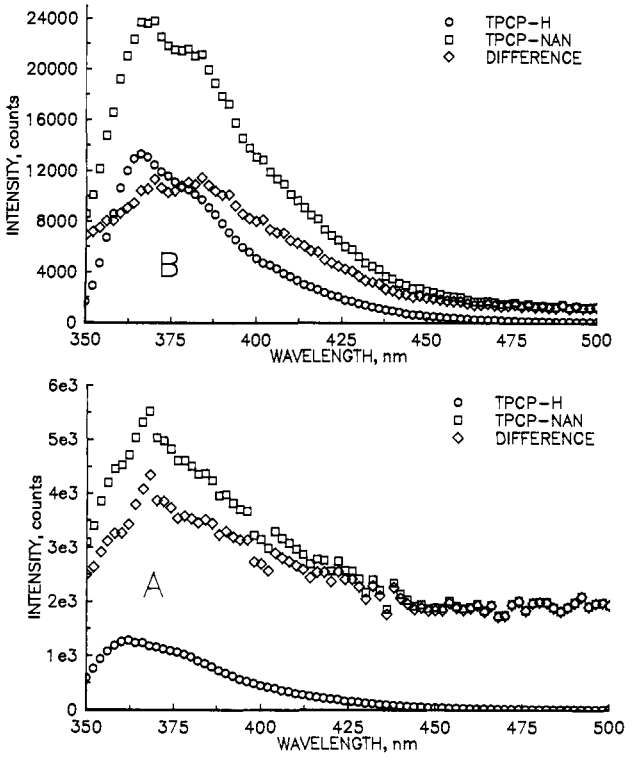

Figure 2. Room temperature fluorescence of TPCP-H and TPCP-NAN in (A) acetonitrile and (B) benzene solution. The intensities of the TPCP-H solutions have been scaled down. Conditions are given in the Experimental Section.

similar primary photoprocesses) and the previously reported studies (i.e., NMR line-broadening analysis, and temperature jump)[1] that were used for slower processes. Transient absorption experiments on **1–6** indicate an interesting sequence of events that ultimately does lead to heterolysis of the C–A bond, albeit as part of a multistep mechanism.

Experimental Section

Preparation of Covalent Precursors. TPCP-H is commercially available (Lancaster Synthesis, Windham, NH) and is the starting material for the preparation of 1,2,3-triphenylcyclopropenium tetrafluoborate.[4] The anion precursors were all commercially available or prepared by published procedures.[1,5] The covalent complexes were prepared by combining equimolar amounts of $TPCP^+$ and the anion in a nonpolar solvent (i.e., ethyl ether or THF), removing the Na^+- or $K^+BF_4^-$ salt by filtration, and recrystallizing the solid that remained after the solvent was removed (typically from hot benzene and hexanes).[1,5]

(4) Dauben, H. J., Jr.; Honnen, L. R.; Harmon, K. M. *J. Org. Chem.* **1960**, *25*, 1442–5.
(5) Molter, K. E. Ph.D. Dissertation, Duke University, Durham, NC, 1988.

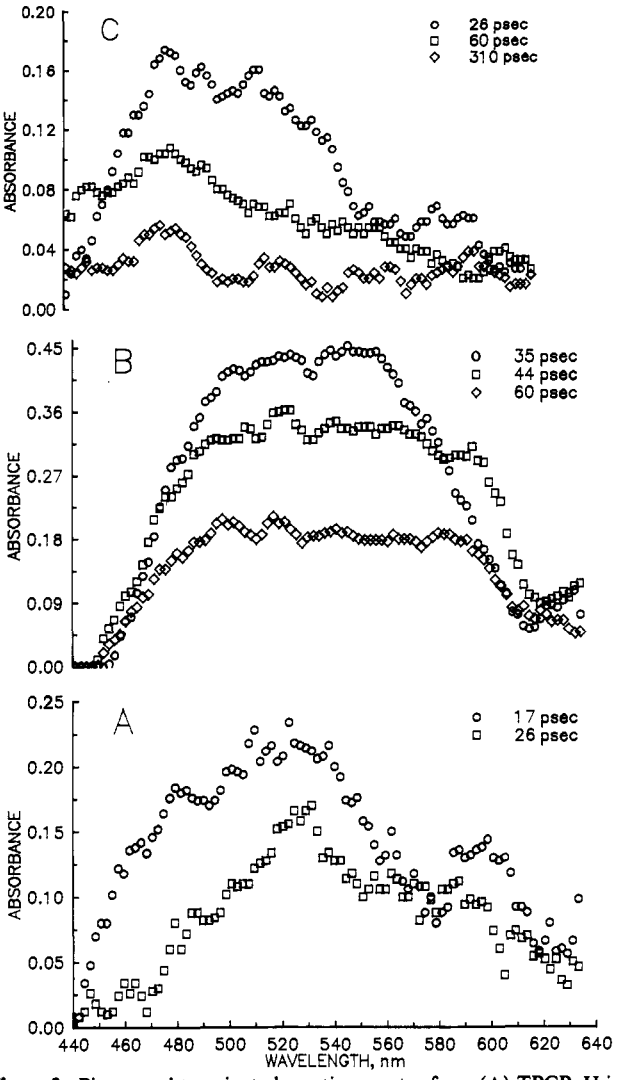

Figure 3. Picosecond transient absorption spectra from (A) TPCP-H in benzene, (B) TPCP-CMN in benzene, and (C) TPCP-CMN in acetonitrile. Spectra are from different, indicated delay times between the arrival of the excitation and probe beam at the sample. For clarity, every fourth point is plotted (see Experimental Section).

Molecular Mechanics Calculations. Molecular mechanics calculations were performed with use of the program PCModel 3.2 (Serena Software, Bloomington, IN). The program was run with all sp^2 atoms configured as "pi atoms," a feature that includes π-VESCF calculations in addition to the use of the MMX (a modified MM2) force field. The data that are reported in Table II are taken from local minima in which the bond from the anion ipso carbon to the incipient anionic center bisects the C1–C3–C2 angle in the cyclopropene. (In all cases, this angle is only approximately bisected. The actual angles are given in Table II, and in some cases the anion bond comes close to aligning with the C1–C3 or C2–C3 bond and not bisecting the angle between them.) Other conformations that represent local minima are ones in which the cyano group or groups are aligned with the cyclopropene (i.e., conformers with the central bond rotated ca. 120° or 240° relative to the one described above). For example, in the case of TPCP–NMN the latter two conformers are ca. 1.8 kcal/mol lower.

Fluorescence. Fluorescence data were recorded on a SPEX Fluorolog-2 emission spectrophotometer equipped with a 450-W Xe lamp and a cooled Hamamatsu R928 photomultiplier tube and have been corrected for instrument response. Samples (ca. 0.5–3 mM in the indicated solvents) were excited at 330 nm. Emission intensities were collected between 350 and 500 nm in 2-nm increments and stored digitally. Figure 2 gives the data from TPCP-NAN and the model TPCP-H in acetonitrile and benzene. In both solvents, TPCP-H gave the more intense fluorescence and that peak was scaled (by 0.015 and 0.1, respectively) and then subtracted from the TPCP-NAN data (in CH_3CN and benzene, respectively).

Picosecond Laser Measurements. A description of the experimental instrumentation has been provided previously.[6] Solutions of the pre-

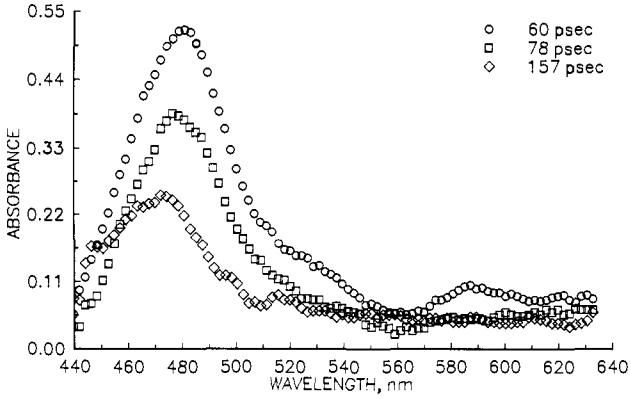

Figure 4. Picosecond transient absorption spectra from TPCP-NAN in acetonitrile. Data are typical of those obtained from all of the nitrophenyl compounds (i.e., TPCP-NMN, TPCP-MET, and TPCP-NAN). Spectra are from different, indicated delay times between the arrival of the excitation and probe beam at the sample. For clarity, every fourth point is plotted (see Experimental Section).

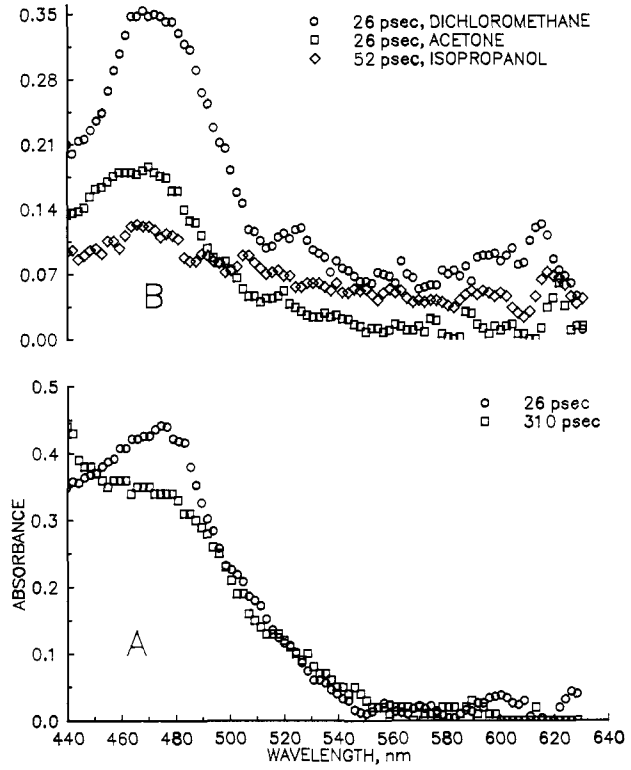

Figure 5. Picosecond transient absorption spectra from (A) TPCP-MET in dichloromethane and (B) TPCP-NAN in dichloromethane, acetone, and 2-propanol. Spectra are from different, indicated delay times between the arrival of the excitation and probe beam at the sample. For clarity, every fourth point is plotted (see Experimental Section).

cursors were prepared so that the optical density (OD) at 355 nm was just greater than 2.0 (ca. 2–6 mM). The laser was operated at 1 Hz, and 500 repetitions were collected and averaged. Observation times were changed by moving a mirror on a micrometer stage or with fiber optic delay lines. The probe light, provided by the continuum generated by 50:50 H_2O/D_2O, was limited to the range 440–640 nm under the configuration used. The ca. 200-nm spectral region was collected and stored digitally as OD, and the spectra in Figures 3–6 represent ca. 350 points each. To improve signal to noise, each five adjacent points were averaged. For clarity in Figures 3–6, only every fourth point is plotted.

Compounds **2–4** dissociate slightly in acetonitrile and other polar solvents.[1] They were irradiated in the presence of 40 mM $TPCP^+BF_4^-$, which shifted the ground-state equilibrium so that, at most, only micromolar quantities of the respective anions are observed at equilibrium. As

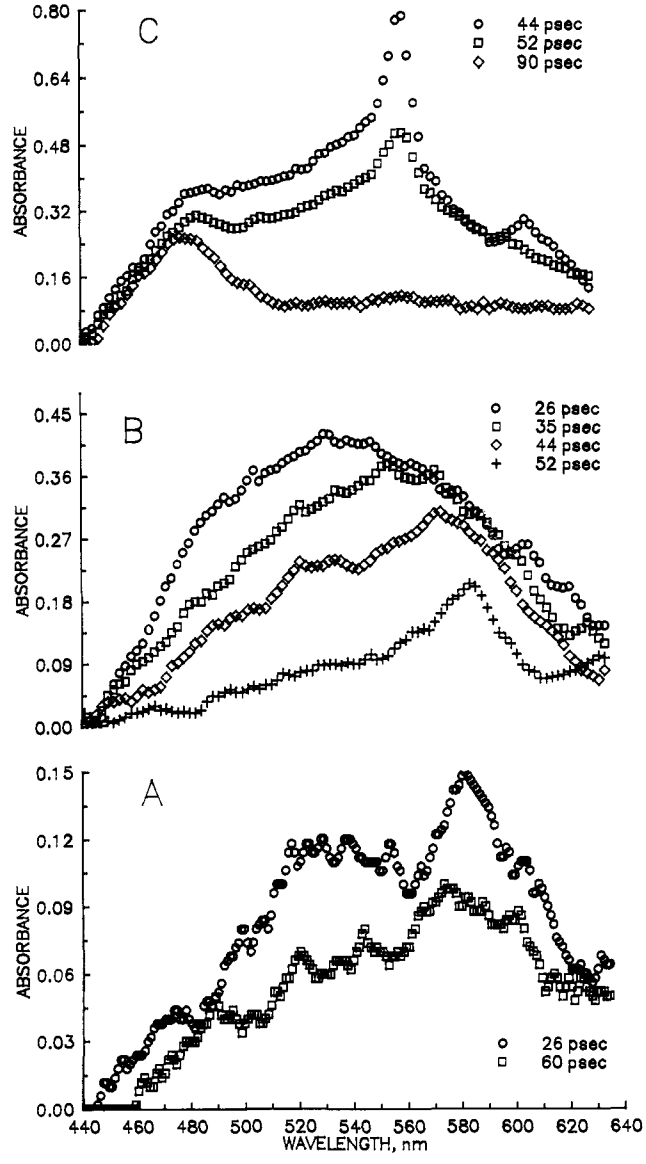

Figure 6. Picosecond transient absorption spectra from TPCP-CFL in (A) benzene, (B) dichloromethane, and (C) acetonitrile. Spectra are from different, indicated delay times between the arrival of the excitation and probe beam at the sample. For clarity, every fourth point is plotted (see Experimental Section).

a control experiment, an acetonitrile solution containing only 20 mM anion (CMN^-, NMN^-, or MET^-) was irradiated, and only massive fluorescence was observed. (No transients in the region 440–640 nm were seen.) Attempts to observe the radical anions from irradiation of ca. 100 mM nitrobenzene, nitrotoluene, benzonitrile, or cyanotoluene with 1 mM stilbene or dimethylaniline did not lead to any transients that could be assigned to the nitroaromatics. (The ground-state absorption of the nitroaromatics of 355 nm at 1.0 M precluded the experiments at those concentrations.)

Nanosecond Laser Measurement. Nanosecond laser transient absorption data were collected with an apparatus that has been described previously.[7] Samples in this study were irradiated with the Nd:YAG third harmonic at 355 nm either parallel or perpendicular to the probe beam (a flashed Xe arc lamp). Samples were prepared in the indicated solvents with 0.5–2 mM precursor (OD of 0.5–1 at 355 nm) and

(6) (a) Simon, J. S.; Peters, K. S. *J. Am. Chem. Soc.* **1981**, *103*, 6403. (b) O'Driscoll, E. D. Ph.D. Dissertation, University of Colorado, Boulder, CO, 1989.

(7) Boyde, S. L.; Strouse, G. F.; Jones, W. E.; Meyer, T. J. *J. Am. Chem. Soc.* **1989**, *111*, 7448–54.

(8) (a) Murov, S. L. *Handbook of Photochemistry*; Marcel Dekker: New York, 1973. (b) *Handbook of Organic Photochemistry*; Scaiano, J. C., Ed.; CRC Press: Boca Raton, FL, 1989; Vols. 1 and 2.

(9) (a) Carmichael, I.; Hug, G. L. *Triplet-Triplet Absorption Spectra of Organic Molecules in Condensed Phases*; Radiation Laboratory, University of Notre Dame: Notre Dame, IN. (b) Carmichael, I.; Hug, G. L. *J. Phys. Chem. Ref. Data* **1986**, *15*, 1. (c) Carmichael, I.; Hug, G. L. In ref 8b, Vol. 1, pp 369–404.

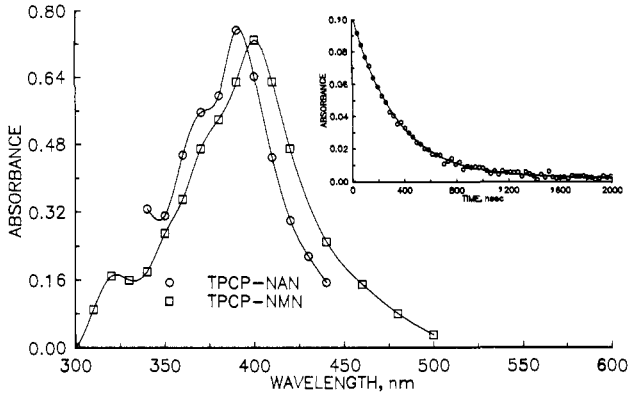

Figure 7. Nanosecond transient absorption spectra from TPCP-NAN and TPCP-NMN in acetonitrile, as indicated. The spectra are obtained from the decay data (at ca. 100 ns) at the indicated wavelengths. The curves drawn through the points are spline fits. The inset shows a typical decay (at 400 nm for TPCP-NAN) with only every second point drawn. The line through the points is the fit to a single exponential obtained by nonlinear regression analysis (see Experimental Section and data in Table III).

Table I. Excited-State Energies and Precursor Redox Potentials

	energy, kcal/mol[a]		absorption maxima, nm[b]		potentials, V[c]	
molecule	E_S	E_T	$S_N \leftarrow S_1$	$T_N \leftarrow T_1$	E_{red}	E_{ox}
TPCP-H	85[d]	60			−1.3[e]	1.5[e]
cis-stilbene	95	57	585	360, 380	−1.8	1.5
nitrobenzene					−0.6	
benzonitrile	104			430, 490	−2.4	
fluorene	95	68		380	−2.4	1.6

[a] Energy of the first singlet (E_S) and triplet (E_T) excited states.[8] [b] Peak maxima for transient absorption from singlet and triplet states, respectively.[9] [c] Half-wave or peak potentials for reduction and oxidation, respectively. (Generally, all are measured in acetonitrile or other polar solvents, relative to SCE.) [d] Estimated in this study from the maxima of the fluorescence of TPCP-H (see text). [e] Measured in this study (peak potentials in acetonitrile containing 50 mM $Bu_4N^+BF_4^-$ as supporting electrolyte; measured at 50 mV/sec relative to Ag/Ag^+ and corrected to SCE as reference).

deaerated by bubbling with N_2 for ca. 15 min. Typically, an entire spectrum was collected at 10- or 20-nm increments, and the rate data in Table III are the averages from such a set of data (generally 10–18 wavelengths for each solution). Individual decays at specific wavelengths are an average of 10 shots, and each contain at least 500 data points. Nonlinear least-squares analyses were performed with use of a Gauss gradient search algorithm for nonlinear regression adapted from a public domain routine (D. Whitman, Cornell University) to DOS-based 386 microcomputers by FK Enterprises (Chapel Hill). A typical decay is shown in the inset to Figure 7. Control experiments identical with the ones described above for the picosecond experiments were also performed.

Results

Structures, Excited States, and Redox Properties of Starting Materials. An analysis of the primary photochemistry must begin with the chromophores on both portions of the covalent precursors and a consideration of some of their properties. The available singlet and triplet excited-state energies and the redox potentials for TPCP-H, *cis*-stilbene, nitrobenzene, benzonitrile, and fluorene (which serve as models for **2–6**) are given in Table I. The chromophores (including the stilbene portion of the TPCP part and the aromatic portions of A) all absorb at 355 nm to varying degrees. (However, TPCP-CMN is the only precursor in which the stilbene absorbs >95% of the light at 355 nm.) In all precursors, the absorption spectra simply appear to be the sum of the two components. For example, spectra obtained from separate solutions of TPCP-H and benzonitrile can be added to yield a result superimposable on the data obtained from TPCP-CMN in the same solvent at the same concentration. Furthermore, the maxima of each component do not shift appreciably as a function of solvent, and thus we believe that we are exciting the same species when we change solvents.

Table II. Data from Structures **2–6** Calculated by Molecular Mechanics

	distance, Å		angle, deg			
compound	central[a]	π[b]	TPCP–[c]	–A[d]	π[e]	dihedral[f]
TPCP-CMN	1.53	2.84	115.7	115.8	51.5	22.7
TPCP-NMN	1.52	2.86	116.0	116.7	52.7	20.8
TPCP-MET	1.52	2.85	116.3	115.7	52.0	17.1
TPCP-NAN	1.52	2.86	117.0	116.5	53.5	16.1
TPCP-CFL	1.53	2.93	117.4	114.6	52.0	1.1

[a] Central bond connecting TPCP to anion (A) portion. [b] Center to center distance from ethenyl carbon of TPCP to ipso carbon of anion (A) π system. [c] Bond angle between cyclopropene plane and central bond. [d] Bond angle between central bond and anion (A) π plane. [e] Bond angle separating the two π planes (sum of the previous two columns minus 180). [f] Dihedral angle formed between the line dissecting the cyclopropene and the ipso to sp^3 carbon bond (CFL has two, all others have one).

The absence of any easily discernable intramolecular charge transfer bands in all cases is surprising if one considers the redox potentials for each pair of components (Table I) but can be rationalized if one simply looks at models of the molecules. Apparently, the π-systems of the two portions are not sufficiently coplanar for the interaction to occur. Some representative data from structures calculated by the molecular mechanics program PCModel 3.2 are given in Table II. The bond angle between the two π systems is greater than 50° in all cases. Even though the minimum distance between one of the ethenyl carbons of TPCP and the closest aromatic carbon on the anionic portion is ca. 3.0 Å and, thus, within their van der Waals radii, the extent of the interaction can only be very minimal (both in terms of the degree and number of atoms overlapping). Absorption from such an EDA complex[10] would not be very intense or shifted very much from the unperturbed system.

Fluorescence Spectra. Room temperature emission spectra were measured for the precursors **1–6** and for a few other compounds in benzene and acetonitrile solutions. Typical spectra are shown in Figure 2. TPCP-H shows a maximum in benzene at 368 nm. When the stilbene is part of a complex like TPCP-NAN, one observes a spectrum that can be separated into two components: one identical with the first (i.e., at 368 nm in benzene) and a second broad one that is slightly red-shifted (maximum at 372 nm). Furthermore, the intensity of the fluorescence from the complex is a factor of ca. 10 times less than equimolar TPCP-H under the same conditions. In addition, the maxima of both components of the spectrum from TPCP-NAN are blue-shifted in acetonitrile relative to the equivalent features in benzene. The relative intensities of the two components from TPCP-NAN are about equal in benzene but favor the longer wavelength, broader one in acetonitrile by ca. 4:1.

We assign the shorter wavelength maxima from the complexes and the peak from TPCP-H to a stilbene singlet fluorescence. This is consistent with *cis*-stilbene emission observed at 360 nm.[11] We assign the second broader feature at longer wavelengths to a conformer of the precursor complexes in which the two π-systems attempt to be coplanar. Since a true exciplex would be a misnomer, we assume that this state is a slightly perturbed singlet of the stilbene in TPCP. The magnitude of the interaction or

(10) For a definition and discussion of EDA complexes, see: *Molecular Association*; Foster, R., Ed.; Academic Press: New York, 1975.
(11) Wintgens, V. In ref 8b, Vol. 1, pp 405–18.
(12) Hamill, W. H. In *Radical Ions*; Kaiser, E. T., Kevan, L., Eds.; Wiley: New York, 1968; pp 321–416.
(13) (a) Goodman, J. L.; Peters, K. S. *J. Am. Chem. Soc.* **1985**, *107*, 1441–2 and 6459. (b) Goodman, J. L.; Peters, K. S. *J. Phys. Chem.* **1986**, *90*, 5506–8. (c) Delcourt, M. O.; Rossi, M. J. *Ibid.* **1982**, *86*, 3233–9.
(14) Tolbert, L. M. In ref 8b, Vol. 2, pp 23–34.
(15) Mecklenburg, S. L.; Hilinski, E. F. *J. Am. Chem. Soc.* **1989**, *111*, 5471–2.
(16) McClelland, R. A.; Mithivanan, N.; Steenken, S. *J. Am. Chem. Soc.* **1990**, *112*, 4857–61.
(17) Freilich, S. Ph.D. Dissertation, Harvard University, Cambridge, MA, 1983.

Table III. Rate Constants for the Decay of ^{3}TPCP[a]

precursor	rate[b] × 10^{-6}, s^{-1}	std dev[c]	conditions
TPCP–CMN	3.2	1.4	acetonitrile
TPCP–NMN	2.0	0.5	acetonitrile
	0.37	0.03	methylene chloride
	0.33	0.03	diethyl ether
	0.47	0.05	ether, 100 mM methanol
	0.60	0.07	benzene
	12.	0.4	benzene, oxygen-saturated
TPCP–NAN	3.5	0.3	acetonitrile
	2.7	0.4	acetonitrile, 0.5 M salt[e]
	1.0	0.08	acetonitrile, 2.0 M salt[e]
	0.36	0.03	methylene chloride
	1.0	0.1	benzene
TPCP–MET	7.1	0.8	acetonitrile
	5.6	0.9	acetonitrile, 0.5 M salt[e]

[a] Transient centered at 400 nm in nanosecond experiments (see text). [b] Values obtained by nonlinear least-squares analysis and averaged for 10–18 different wavelengths. [c] Standard deviation from the average in the previous column. [d] Solutions are ca. 3–6 mM precursor in indicated solvent, deaerated with nitrogen. [e] Tetrabutylammonium fluoborate added to increase ionic strength.

perturbation can be estimated from the shift of the maximum (e.g., for TPCP–NAN in benzene from 368 to 372 nm and in acetonitrile from 364 to 370 nm) and is on the order of only 1 kcal/mol.

Picosecond Transient Absorption Studies. The results from irradiation of the precursors **1–6** can be seen in Figures 3–6. Figure 3A and B contains spectra from the irradiation of TPCP–H and TPCP–CMN in benzene, respectively. Both yield the same transient centered at ca. 545 nm, a result consistent with the stilbene of the TPCP absorbing all of the light. (Another small peak at 580–600 nm is apparent at early times.) Figure 3C is the spectrum from TPCP–CMN in acetonitrile; it contains a peak centered at 485 nm with only a hint of the absorbance at 545 nm. Figure 4 contains a typical set of spectra from TPCP–NAN that is representative of all of the ones from the precursors with a nitrophenyl chromophore (i.e., TPCP–NMN, TPCP–MET, and TPCP–NAN) irradiated in acetonitrile solutions. All of them give the same peak, centered at 485 nm (Figure 4), but give no transients in benzene solution. (Results are not shown.) Furthermore, the spectra in Figures 3C and 4 appear to be the same.

Figure 5 contains the spectra from TPCP–MET in methylene chloride as A and TPCP–NAN in polar solvents as B. Again, the spectral feature at 485 nm is the same with the notable difference that, for TPCP–MET (Figure 5A), it is superimposed on an absorbance at shorter wavelengths (whose maximum cannot be detected under the experimental conditions), which appears to maximize on the scale of hundreds of picoseconds. Further evidence for it appears in the next section outlining the nanosecond transient absorption results. Figure 5B contains spectra from TPCP–NAN in three polar solvents, all showing the feature at ca. 485 nm and indicating that the solvent may have a substantial effect on the transient's growth and/or decay kinetics.

Figure 6 shows the transient spectra obtained from TPCP–CFL in benzene (A), methylene chloride (B), and acetonitrile (C). Both the fluorene and stilbene chromophores absorb at 355 nm, although the singlet energy of TPCP–H (ca. 85 kcal/mol) is less than that of fluorene (ca. 95 kcal/mol). The spectrum in benzene has features at 540 and 580 nm. The one in CH_2Cl_2 is a very broad peak at early times that appears (as a result of time evolution) to be comprised of two components, one at 585 nm and another at shorter wavelengths whose maximum is not exactly discernable. The spectrum in acetonitrile is clearly composed of two features, at 480 and 555 nm.

Nanosecond Transient Absorption Studies. Irradiation of all precursors **2–6** under virtually all conditions (air-saturated or degassed solutions in benzene, methylene chloride, or acetonitrile) give transients that have identical spectra, peaks centered at ca. 400 nm, which decay by first-order kinetics. Two typical spectra are shown in Figure 7. The time evolution of the absorbance decay is shown as an inset to Figure 7, and the rate constants obtained by nonlinear least-squares fits are contained in Table III. Those rates do not depend greatly on the nature of the solvent, but the transient (i.e., the 400-nm peak) appears to react readily with oxygen. For example, the absorbance from TPCP–NMN in benzene decays with an observed rate constant of 6×10^5 s^{-1} in deaerated benzene but 1.2×10^7 s^{-1} in oxygen-saturated benzene. On the basis of these two data points, this suggests a bimolecular rate constant of ca. 1×10^9 M^{-1} s^{-1}, a value approaching diffusion control.)

Besides the common intermediate at 400 nm, several of the precursors yield a second peak apparently superimposed over the first feature. Thus, TPCP–NMN and TPCP–NAN yield the spectra shown in Figures 8 and 9, respectively. Clearer (but

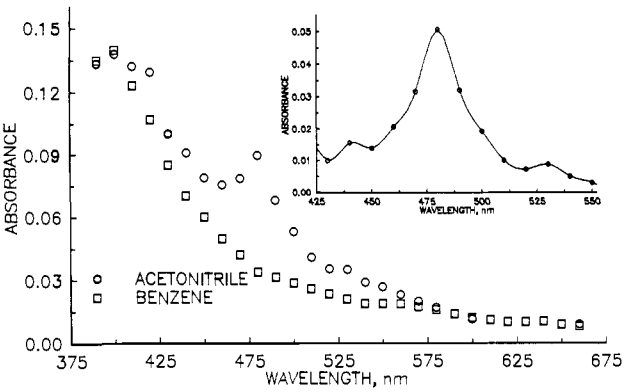

Figure 8. Nanosecond transient absorption spectra from 2 mM TPCP–NMN in acetonitrile and benzene, as indicated. The acetonitrile solution contains 40 mM $TPCP^+BF_4^-$ to retard dissociation in the ground state. The inset shows a region of the difference spectrum. The line drawn through the points is a spline fit.

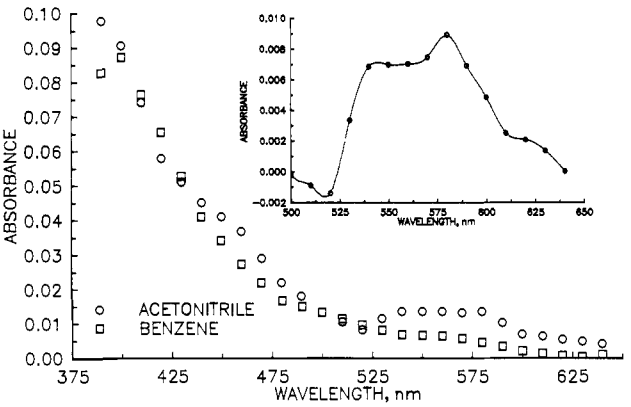

Figure 9. Nanosecond transient absorption spectra from 2 mM TPCP–NAN in acetonitrile and benzene, as indicated. The acetonitrile solution contains 0.5 M $(n\text{-Bu})_4N^+BF_4^-$ added to induce ion formation. The inset shows a region of the difference spectrum. The line drawn through the points is a spline fit. The spectrum for authentic NMN^- is also broad with structural features.

Table IV. Transient Absorption Peak Maxima[a]

R–H	$RH^{\bullet+}$	$RH^{\bullet-}$	R^+	R^-
TPCP–H	485[b]	485[b]	325[c]	
stilbene	475,[d] 510[e]	*f*		
CMN–H				358[c]
NMN–H				478[c]
MET–H				495[c]
NAN–H				530–70[c]
fluorene	640[g]	560[h]	488,[i] 515[j]	

[a] Maximum of longest wavelength peak (nm). [b] Measured in this study from intermolecular electron transfer with another molecule of TPCP–H (see Discussion). [c] Measured with use of starting, stable ions.[1,5] [d] From *trans*-stilbene.[12,13] [e] From *cis*-stilbene.[12] [f] Same as the radical cation.[12] [g] From fluorene,[14] 9-fluorenol,[15,16] or 9-methyl-9-fluorenol.[15] [h] From fluorene.[17] [i] From 9-methyl-9-fluorenol.[15] [j] From 9-fluorenol.[15]

noisier) views of these transients are the difference spectra shown in the insets (with a spline-fit line drawn through the points). These species have maxima that correspond to the respective anions, NMN^- at 480 nm and NAN^- at 530–70 nm (see Table IV).

Discussion

Photolysis and the Primary Event. The irradiation of precursors **1–6** leads to a multistep sequence of events, but one that can be easily rationalized in terms of previously well-studied, single events. The absence of charge-transfer bands in the absorption spectra ($S_1 \leftarrow S_0$) of **1–6** and the fluorescence data suggest that we should be populating excited states associated with localized chromophores (i.e., the stilbene of TPCP or the aryl part of A). This is supported by the nature of the fluorescence from the precursors: One part is identical with unperturbed TPCP, and a second is due to a conformer in which the two π-systems interact, albeit quite minimally. It is not likely that the second, broader emission is due to the triplet (since the emission was measured at room temperature, and the triplet energies would be much lower) or a delayed fluorescence from an event like radical ion pair annihilation (since the radical ion pairs in general are at much lower energies than the singlet excited states). We conclude that the primary photochemical event must be the production of an excited singlet state of the stilbene in TPCP or the aryl part of the other half. The photochemistry of cyclopropene derivatives has been reviewed,[18] and previous reports include the dimerization of TPCP–H (**1**) and 3-carbomethoxy-1,2-diphenylcyclopropene.[19]

The picosecond spectra from TPCP–H and TPCP–CMN solutions in benzene (Figure 3A and B) are assigned to ^{1}TPCP and thus support the contention that the primary event is population of a localized singlet excited state. The assignment of this peak at 545 nm to ^{1}TPCP is consistent with the data for *cis*- and *trans*-stilbene. In addition, the earliest spectra from TPCP–CFL in benzene and CH_2Cl_2 (Figure 6A and B) have two components, one at 580 nm and a second at shorter wavelengths that could be assigned to a peak at 545 nm. Those maxima correspond to ^{1}CFL (580 nm, Table I) and ^{1}TPCP (545 nm). The S_1 states of nitrobenzene (or nitrotoluene) and benzonitrile (or cyanotoluene) would be expected at wavelengths below 440 nm (i.e., one of our detection limits), and indeed irradiation of these model compounds under experimental conditions produced no transients in the region 440–640 nm.

In summary, we observe ^{1}TPCP when the stilbene absorbs all or at least part of the light. Likewise, we see ^{1}CFL when it absorbs at least part of the light. However, we observe no excited states when nitrophenyl is the primary chromophore, apparently because we do not have access to the appropriate spectral region or because those excited states are too short lived (or both).

Secondary Event: Electron Transfer. The redox properties of the chromophores ($E_{ox} - E_{red}$, Table I) can be used to predict the propensity of any pair (1) to form EDA complexes when used in conjunction with emission data[20] or (2) to undergo electron transfer after excitation.[21] Although the geometric constraints of the molecules prevented their forming intramolecular EDA complexes,[22] electron transfer is not prohibited. Furthermore, the electron transfer might well be expected independent of which conformation is favored in the precursor ground state. However, once electron transfer has occurred, the geometric constraints would be expected to have a substantial effect on the energetics of the radical ion pair, which would not be able to achieve optimal stabilization by formation of a contact radical ion pair.

The energies of the appropriate excited states are sufficient to make the redox reaction at least moderately exothermic. We suggest that radical ion pair formation explains the picosecond spectra in polar solvents. Thus, we observe a common peak at the earliest observation times in Figures 3C, 4, 5, and 6C at 485 nm, which we assign to $TPCP^{\bullet+}$, a result consistent with the spectral features of stilbenyl radical cations (Table IV). A peak with the same features can be obtained from the irradiation of 30 mM TPCP–H in acetonitrile. Apparently, in that case, TPCP–H serves both as the electron donor and acceptor and the resulting spectrum is a superposition of $TPCP^{\bullet+}$ and $TPCP^{\bullet-}$. The formation and reactions of the radical cation of stilbene by intermolecular photoinduced electron transfer via picosecond techniques have been previously investigated.[13]

The case of TPCP–CFL requires and enables a more complete analysis. Electron transfer presumably can occur in two directions from either localized excited state (represented as [TPCP–CFL]* below):

$$[\text{TPCP–CFL}]^* \rightarrow {}^{+\bullet}\text{TPCP–CFL}^{\bullet-} \qquad E_{ox} - E_{red} = 3.9 \text{ V (90 kcal/mol)} \quad (1)$$

$$[\text{TPCP–CFL}]^* \rightarrow {}^{\bullet}\text{TPCP–CFL}^{\bullet+} \qquad E_{ox} - E_{red} = 2.9 \text{ V (78 kcal/mol)} \quad (2)$$

The redox potentials are based on TPCP–H and fluorene as a model for CFL (Table I). The 9-cyano substituent in CFL might exert an electronic effect even though it is attached at an sp^3 carbon. That would serve to lower E_{red} and raise E_{ox} of 9-cyanofluorene relative to fluorene itself. The outcome on the equations above would be to lower the value from the first one and raise the value of the second. This must be the case since we observe peaks at 485 and 555 nm in acetonitrile, and according to the values in Table IV those correspond to the radical ion pair described in eq 1 above.

Thus, we observe a common intermediate in polar solvents from all precursors (i.e., at 485 nm) and assign it to the $TPCP^{\bullet+}$ portion. We observed and assigned a peak at 555 nm to the $CFL^{\bullet-}$ portion. The nitro- and cyanophenyl radical anions are apparently not spectrally accessible.

Radical Ion Pair Decay: Back Electron Transfer and Bond Fragmentation. Intramolecular electron transfer has been well-studied, including aspects concerning (1) the effect of geometry on the rates[23] and (2) the role of σ-bond spacers.[24] Stilbenes and electron-deficient aromatics have played an integral part of the development of the general area,[25] and their involvement in electron transfer here is no surprise. Bimolecular photochemical reactions of stilbenes (with alkenes, dienes, amines, and protic solvents) have been reviewed by Lewis,[26] as have stilbene electron-transfer chemistry[27] and the involvement of stilbene exciplexes.[28] There are two reports of photoinduced electron-transfer chemistry of analogues of TPCP. Padwa and co-workers report the ring expansion of a series of 3-(3′-propenyl)-1,2-diphenylcyclopropenes in the presence of 9,10-dicyanoanthracene (DCA) that ultimately produce trisubstituted benzenes.[29] Farid and

(18) Padwa, A. *Acc. Chem. Res.* **1979**, *12*, 310–7.
(19) DeBoer, C. D.; Wadsworth, D. H.; Perkins, W. C. *J. Am. Chem. Soc.* **1973**, *95*, 861–9.
(20) Weller, A. In *The Exciplex*; Gordon, M.; Ware, W. R., Eds.; Academic Press: New York, 1973; pp 23–38.
(21) (a) Rehm, D.; Weller, A. *Isr. J. Chem.* **1970**, *8*, 259. (b) Weller, A. *Z. Phys. Chem. (Wiesbaden)* **1982**, *133*, 93. (c) Suppan, P.; Vauthey, E. *Photochem. Photobiol.* **1989**, *49*, 239.
(22) Intramolecular EDA complexes have been observed in many cases especially when the number of carbons connecting the aromatic systems is three or four. This is often referred to as Hirayama's rule: Hirayama, F. *J. Chem. Phys.* **1965**, *42*, 3163.
(23) For a discussion concerning the current understanding of electron-transfer photophysics and models that describe it, see: (a) Closs, G. L.; Johnson, M. D.; Miller, J. R.; Piotrowiak, P. *J. Am. Chem. Soc.* **1989**, *111*, 3751–3. (b) Closs, G. L.; Miller, J. R. *Science (Washington, D.C.)* **1988**, *240*, 440–7. (c) Miller, J. R.; Calcaterra, L. T.; Closs, G. L. *J. Am. Chem. Soc.* **1984**, *106*, 3047–9. (d) McIntosh, A. R.; Siemiarczuk, A.; Bolton, J. R.; Stillman, M. J.; Ho, T. F.; Weedon, A. C. *Ibid.* **1983**, *105*, 7215. (e) Mataga, N.; Karen, A.; Okada, T.; Nishitani, S.; Kurata, N.; Sakata, Y.; Misumi, S. *Ibid.* **1984**, *106*, 2442. (f) Pasman, P.; Mes, G. F.; Koper, N. W.; Verhoeven. J. W. *Ibid.* **1985**, *107*, 5839.
(24) Miller, J. R. *Nouv. J. Chem.* **1987**, *11*, 83–90.
(25) For numerous examples, see: Fox, M. A., Chanon, M., Eds. *Photoinduced Electron Transfer.* Part C. Photoinduced Electron Transfer Reactions: Organic Substrates; Elsevier: Amsterdam, 1988.
(26) Lewis, F. D. *Adv. Photochem.* **1986**, *13*, 165–235.
(27) Lewis, F. D. In ref 25, pp 1–69.
(28) Lewis, F. D. *Acc. Chem. Res.* **1979**, *12*, 152–8.
(29) Padwa, A.; Chou, C. S.; Rieker, W. F. *J. Org. Chem.* **1980**, *45*, 4555.

co-workers report dimer formation from the radical cation of 3-carbomethoxy-1,2-diphenylcyclopropene (formed with DCA) or the triplet stilbene that results from back electron transfer within the stilbene–DCA radical ion pair.[30] This latter report is similar to some of the present study since back electron transfer competes with chemistry produced from the stilbenyl radical cation. However, the use of intramolecular radical ion pairs to effect C–C bond fragmentation in the present study is novel to the best of our knowledge.

Further details elucidating the behavior of the intramolecular radical ion pairs comes from the nanosecond transient absorption data. The observation of the peak centered at ca. 400 nm from irradiation of all complexes **2–6** under a variety of conditions suggests a TPCP-centered species, since this is the only structural feature in common. The kinetic observations (Table III) lead us to assign it as ^{3}TPCP. It has a lifetime in the microseconds, reacts with oxygen at nearly diffusion-controlled rates, and does not disappear appreciably faster when 100 mM methanol is added to ether solutions ($k_Q < 1 \times 10^6$ based on two points). The peak maximum at 400 nm is consistent with ^{3}stilbene, which has been observed at ca. 380 nm (Table I). TPCP has the lowest triplet energy of all of the chromophores in use (Table I). The decay of the transient at 400 nm is not effected by (n-Bu)$_3$SnH even at concentrations as high as 0.15 M. The use of 5-methyl-1,3-hexadiene as a quencher reduces both the intensity of the 400-nm transient and its lifetime. Although Stern–Volmer plots of the intensity or lifetime versus diene concentration are both markedly nonlinear, we have used the slopes from the low diene concentration, linear portions to make some estimates. From the change in the decay rate (slope ca. 0.52), we conclude that the diene triplet energy (E_T = ca. 59 kcal/mol) is not sufficiently lower than that of ^{3}TPCP (k_Q = ca. 1–2 × 10^6 M^{-1} s^{-1}). The slope of the linear part of the Stern–Volmer quenching of the 400-nm intensity is ca. 5.7 and thus indicates that dienes are very good quenchers of one of the precursors to the triplet. Since dienes react quite readily with stilbene radical cations,[26,27] it seems most likely that they are intercepting the radical ion pair at a rate ca. 5.7 times its normal decay. The rapid decay of the radical ion pair (ca. 7 × 10^9 s^{-1}, see Figure 4 for an example) suggests that the reaction with the dienes is diffusion-controlled. (The difficulty in finding triplet quenchers of the appropriate energy that also have the correct redox properties, extinction coefficients, and similar requirements encouraged us to abandon this kind of study.)

Furthermore, the observation of ^{3}TPCP can easily be explained as a consequence of the back electron transfer within the intramolecular radical ion pair. Analogous intermolecular chemistry was reported by Farid.[30] The energy of the ion pair $^{+\bullet}$TPCP–A$^{\bullet-}$ can be estimated from the redox potentials in Table I for A = CMN (3.9 V or 90 kcal/mol), NMN, MET, or NAN (2.7 V or 62 kcal/mol), and CFL (<3.9 V or 90 kcal/mol, eq 1 and related discussion). By those estimates, all radical ion pair energies occur above those of ^{3}TPCP (at ca. 60 kcal/mol, see Table I), although the nitrophenyl series (i.e., NMN, MET, and NAN) are virtually isoenergetic.

It is in the nitrophenyl cases that additional transients are observed in polar solvents on the nanosecond time scale (see Figures 8 and 9). Thus, TPCP–NMN yields a peak at 480 nm, and TPCP–NAN produces some features at 530–70 nm. These have been assigned to NMN$^-$ and NAN$^-$ and are superimposable with spectra obtained from authentic samples of the anions used to make the covalent precursors. The TPCP$^+$ that would be expected from the heterolysis of the central bond absorbs at 325 nm, a wavelength not easily accessible in the experiments.[31]

Formation of Ion Pairs from Radical Ion Pairs. Although one can make a case for the existence of closed-shell ions (C$^+$, A$^-$) in the nanosecond spectra (Figures 8 and 9), their presence is not conclusive from the picosecond data. This is due, at least in part, to the observation of other transients in the same spectral regions. Since radical ion pair formation is obvious within the time scale of the exciting beam (ca. 25 ps), we would anticipate that central bond breaking could also begin to occur at that time. Heterolysis of that bond should lead to a pair of ions in close proximity that are solvated in a manner optimal for the radical ion pair. One would expect that very little nuclear motion would be necessary to produce the contact ion pair. This in turn would begin a sequence of events for the ions. Thus, the contact ion pair can recombine or diffuse apart to form solvent-separated and ultimately free ions, although the absorbance that we observe (due to the anion) would not be able to distinguish these mechanistic features. The decay of the anion absorbances from the nanosecond experiments (Figures 8 and 9) appear to fit pseudo-first-order kinetics (because of the added TPCP$^+$BF$_4^-$), and have rates about 1 order of magnitude slower than those of ^{3}TPCP.[32] The agreement of the rate of disappearance of NMN$^-$ from this study (3.7 × 10^6 M^{-1} s^{-1}) with the rate of coordination of NMN$^-$ from temperature jump experiments at high salt concentration (1.63 × 10^6 M^{-1} s^{-1}) is very encouraging.

Scheme II. Fragmentation of Radical Ion Pair to Radicals or Ions

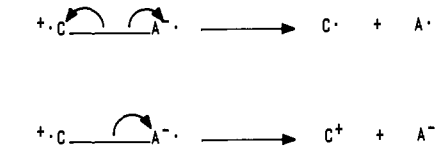

The optical density (and thus the amounts) of the anions NMN$^-$ and NAN$^-$ observed at early times in the nanosecond experiments (at ca. 100 ns) can be increased by the addition of a nonreactive salt like tetrabutylammonium fluoborate, which we believe simply serves to increase the solvent polarity. The increased fragmentation may be due to an increment in the amount of heterolysis of the radical ion pair or simply to more anions escaping the solvent cage once the ion pairs are formed. The limited data from these systems do not allow us to differentiate at this time.

No evidence is observed for any anions from TPCP–CMN and TPCP–CFL. The anion CMN$^-$ absorbs in a spectral region (ca. 360 nm) at which it is difficult to detect under the experimental conditions.[31] However, both CMN$^-$ and CFL$^-$ (which absorb in the visible) would be formed from radical ion pairs whose energies are much higher than that of ^{3}TPCP. For these examples, the back electron transfer rate may be much faster than bond heterolysis. Alternatively, recombination of the contact ion pair may be extremely efficient and, thus, prevent any solvent cage escape.

The lack of ions from TPCP–MET is somewhat puzzling at first. The energetics from our model systems would predict that it should behave like its isomer TPCP–NMN. However, it is obvious that the kinetics are quite different. One can see the rise of a shorter wavelength peak from TPCP–MET in the 310-ps spectrum in Figure 5A that is not observed in the data from TPCP–NMN in CH_2Cl_2 or CH_3CN (not shown). We tentatively assign that peak to ^{3}TPCP, observed as a maximum at ca. 400 nm in the nanosecond data. This implies that back electron transfer is very rapid in the meta isomer and that central bond fragmentation may not favorably compete.

Fragmentation of bonds has been observed in radical cations and radical anions (separately) when those species have been prepared chemically, electrochemically, or by photoinduced electron transfer. Thus, radical cations of 1,2-diaryl-substituted ethanes, each cleaving to yield a cation and radical product, have

(30) Brown-Wensley, K. A.; Mattes, S. L.; Farid, S. *J. Am. Chem. Soc.* **1978**, *100*, 4162–72.

(31) Besides being close to the irradiation wavelength at 355 nm, a number of species all absorb this far into the ultraviolet. In addition, the sample solution generally has an OD > 1 at wavelengths < ca. 340 nm since the OD at 355 nm is chosen to be between 0.5 and 1.

(32) For example, in the range 430–530 nm, the decay from TPCP–NMN (Figure 8) can be fit to two exponentials: 2.35 × 10^6 s^{-1} and 1.5 × 10^5 s^{-1}. The first has been assigned to ^{3}TPCP decay and is consistent with decays obtained from the same sample but at wavelengths where the triplet absorption is dominant (ca. 400 nm). If one converts the slower rate to second-order (by using the TPCP$^+$ concentration of 40 mM that had been added to prevent dissociation of the ground-state complex), one obtains a rate of 3.7 × 10^6 M^{-1} s^{-1}. That number is in very good agreement for the second-order rate reported for the coordination of TPCP$^+$ with NMN$^-$ in acetonitrile containing 0.48 M Bu$_4$N$^+$BF$_4^-$ (1.63 × 10^6 M^{-1} s^{-1}; ref 1f).

Scheme III. Mechanism Relating Various Intermediates

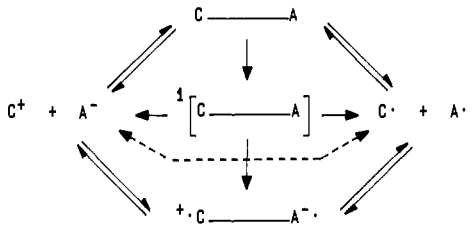

been observed by Trahanovsky,[33] Griffin,[34] and Das.[35] Related aminium radicals (i.e., 1,2-diaryl-substituted aminomethanes $Ar^1CH_2NAr^2$) have been studied systematically by Whitten.[36] The analogous behavior of radical anions and dianions of diaryl-substituted ethanes is also being investigated.[37] Of course, the radical anions each produce an anion and a radical.

Radical ion pairs of the kind described herein (and related ones) can, in principle, cleave to yield either a pair of ions or neutral radicals. This is easy to describe (on paper, at least) in terms of electron "pushing". If one apportions one electron of the central bond to each of the two parts, the result is the radical pair. Alternatively, when the central bond electron pair is shifted to the radical anion part, the closed-shell ion pair results. The partitioning to yield neutral radicals or ions can be seen in Scheme II. A few modifications and additions to Scheme I yield a complex mechanism in Scheme III.

One would anticipate that, with all of the various energy surfaces interwoven mechanistically, one should eventually reach the bottom of the energy scale. That suggests that the ion pair is more thermodynamically stable than the radical pair for the systems in which we observe ions. That hypothesis is true for the precursors **2–6**, and it can be easily shown for these and other related molecules. Electrochemical potentials for the reduction of $TPCP^+$ [38] and oxidation of stable anions[39] enable a prediction of whether the ion pair or radical pair are favored at equilibrium. The ions (C^+, A^-) are all thermodynamically favored (>10 kcal/mol) over the radicals ($C^\bullet$, $A^\bullet$) for the cases **2–6**.[40]

An alternative should be considered at this point. One possibility is that the chromophore-localized excited states give rise to the central bond heterolysis and the ions directly (in competition with electron transfer). The electron transfer occurs within the duration of the pulse in polar solvents (< ca. 25 ps; see Figures 3C, 4, 5, and 6C). One would expect to see anions at these early times in that case. In particular, one should see NAN^- at 530 nm. (NMN^- occurs at 478 nm and overlaps with $TPCP^{\bullet+}$.) Furthermore, we do not observe ionic products under circumstances where no radical ions are formed. For example, we see no ions from TPCP–NMN or TPCP–NAN in benzene. Although one might argue that the nonpolar solvent does not favor their formation, we do not have even the hint of evidence for short-lived contact ion pairs at the earliest times in the picosecond experiments. Therefore, we suggest that the ions come from the radical ions. More direct evidence (for example, being able to measure the rise time of the anions) would make this point more unequivocally, and the question is being pursued in related systems.

Another matter has to do with the efficiency of the central bond cleavage. Two mechanistic extremes should be considered, those of thermodynamic or kinetic control. Data are available from calorimetrically determined heats of reaction for the combination of $TPCP^+$ and a variety of anions.[1] Thus, the enthalpy of heterolysis (eq 3) is the negative of the measured heat of combination:

$$\text{TPCP–A} \rightarrow \text{TPCP}^+ + \text{A}^- \qquad \Delta H_{\text{hetero}} = -\Delta H_{\text{combn}} \quad (3)$$

$$^{\bullet+}\text{TPCP–A}^{\bullet-} \rightarrow \text{TPCP–A} \qquad \Delta G_{\text{eq 4}} = -(E_{\text{ox}} - E_{\text{red}}) \quad (4)$$

$$^{\bullet+}\text{TPCP–A}^{\bullet-} \rightarrow \text{TPCP}^+ + \text{A}^- \qquad \Delta G_{\text{eq 5}} \quad (5)$$

The measured enthalpies and calculated free energies are given in Table V.[41] The free energies for production of the radical ion pairs (i.e., the reverse of eq 4) can be calculated from the redox potentials in Table I and are given in Table V. Thus, one can construct a thermodynamic cycle by adding eq 3 (after converting to free energy values)[41] and eq 4 to estimate the free energy of heterolysis of the radical ion pair (eq 5). These reactions are all predicted to be very exothermic (last column, Table V) even if one takes into account considerable error in these estimates. Since we observe ions from the first and last entries in Table V (i.e., TPCP–NMN and TPCP–NAN), which predict one of the most and the least exothermic reactions (eq 5), simple thermodynamic control must not be in effect. That suggests kinetic control. The simplest scheme for kinetic control is one in which the radical ion pair partitions between back electron transfer and bond heterolysis. Back electron transfer to form ^{3}TPCP would be very fast in the cases of TPCP–CMN and TPCP–CFL where that process is exothermic by ca. 30 kcal/mol. In the nitrophenyl series, that process is only exothermic by a few kilocalories per mole. Nonetheless, growth of the triplet is quite fast even in these cases. One can see that from the shorter wavelength peak from TPCP–MET (Figure 5A), which grows in on the order of hundreds of picoseconds.

The possibility exists that the nanosecond laser transient experiments in which closed-shell ions are observed (Figures 8 and 9) give rise to those ions by a photochemically induced temperature jump. In other words, the laser could produce a local temperature rise in which a thermal heterolysis could occur. One can dismiss

Table V. Measured Enthalpies and Calculated Free Energies

	TPCP–A → $TPCP^+ + A^-$		TPCP → $^{\bullet+}$TPCP–$A^{\bullet-}$		$^{\bullet+}$TPCP–$A^{\bullet-}$ → $TPCP^+ + A^-$
A	$\Delta H_{\text{heterol}}$[a,b]	$\Delta G_{\text{heterol}}$[a,b]	$E_{\text{ox}} - E_{\text{red}}$[c]	ΔG	ΔG
NMN	~10	~6	2.7	~62	~−56
MET	~10	~6	2.7	~62	~−56
CMN	10.0	6	3.9	90	−84
CFL	19.6	16	<3.9	<90	<−74
NAN	~53	~49	2.7	62	~−13

[a] In kilocalories per mole. [b] Enthalpy of heterolysis is the negative of the measured heat of combination.[1] Free energy is determined by correcting for the entropy change ($T\Delta S$ = 4 kcal/mol is assumed).[41] [c] Volts versus SCE (see Table I). [d] From eq 4 (see text). [e] From eq 5 (column 2 − column 4, in this table).

(33) Trahanovsky, W. S.; Brixius, D. W. *J. Am. Chem. Soc.* **1973**, *95*, 6778–80.

(34) (a) Griffin, G. W.; Wong, J. P. K.; Fahmi, A. A. *J. Photochem.* **1981**, *17*, 104. (b) Wong, J. P. K.; Fahmi, A. A.; Griffin, G. W.; Bhacca, N. S. *Tetrahedron* **1981**, *37*, 3345–55.

(35) Reichel, L. W.; Griffin, G. W.; Muller, A. J.; Das, P. K.; Ege, S. N. *Can. J. Chem.* **1984**, *62*, 424–36.

(36) (a) Lee, L. Y. C.; Ci, X.; Giannotti, C.; Whitten, D. G. *J. Am. Chem. Soc.* **1986**, *108*, 175–7. (b) Lee, L. Y. C.; Ci, X.; Whitten, D. G. *Ibid.* **1987**, *109*, 2536–8 and 7215–7. (c) Ci, X.; Whitten, D. G. In ref 25, pp 553–77. (d) Ci, X.; da Silva, R. S.; Nicodem, D.; Whitten, D. G. *Ibid.* **1989**, *111*, 1337–43. (e) Kellett, M. A.; Whitten, D. G. *Ibid.* **1989**, *111*, 2314–6. (f) Ci, X.; Whitten, D. G. *Ibid.* **1989**, *111*, 3459–61. (g) Haugen, C. M.; Whitten, D. G. *Ibid.* **1989**, *111*, 7281–2.

(37) (a) Patel, K. M.; Baltisberger, R. J.; Stenberg, V. I.; Woolsey, N. F. *J. Org. Chem.* **1982**, *47*, 4250. (b) Beak, P.; Sullivan, T. A. *J. Am. Chem. Soc.* **1982**, *104*, 4450. (c) Koppang, M.; Woolsey, N. F.; Bartak, D. E. *Ibid.* **1984**, *106*, 2799. (d) Andrieux, C. P.; Gallardo, I.; Saveant, J.-M.; Su, K.-B. *Ibid.* **1986**, *108*, 638 and references cited therein. (e) Saeva, F. *Tetrahedron* **1986**, *42*, 6132. (f) Dewald, R. R.; Conlon, N. J.; Song, W. M. *J. Org. Chem.* **1989**, *54*, 261. (g) Maslak, P.; Narvaez, J. N.; Kula, J.; Malinski, D. S. *Ibid.* **1990**, *55*, 4550–9 and references cited therein.

(38) Breslow, R.; Chu, W. *J. Am. Chem. Soc.* **1973**, *95*, 411.

(39) Bordwell, F. G.; Bausch, M. J. *J. Am. Chem. Soc.* **1986**, *108*, 1979.

(40) The reduction potential for $TPCP^+BF_4^-$ is 0.72 V vs SCE (ref 38). The oxidation potentials ($A^- \rightarrow A^\bullet$) for some of the anions have been determined or can be estimated from data in ref 39: NMN^-, 0.53 V vs SCE; CMN^-, 0.45 V vs SCE; and NAN^-, 0.23 V vs SCE. They were reported versus the ferrocene/ferrocinium couple and have been converted to the SCE reference by correcting for the ferrocene redox (0.35 V vs SCE): Kotz, J. C. In *Topics in Organic Electrochemistry*; Fry, A. J., Britton, W. E., Eds.; Plenum Press: New York, 1986; p 85.

(41) The heterolysis (eq 3) generates two fragments from the starting material and, thus, would have a substantial positive entropy. For examples, see: Lowry, T. H.; Richardson, K. S. *Mechanism and Theory in Organic Chemistry*, 3rd ed.; Harper & Row: New York, 1987; pp 163–77. Thus, the free energy of heterolysis would be more exothermic than the enthalpy by another 4–6 kcal/mol at room temperature.

this possibility with a few calculations.[42] The data in Figure 9 predict a temperature jump of ca. 64 °C, while the complete laser power used can account for only a maximum of ca. 6 °C. The closed-shell anions clearly must be generated by a photochemical event, and we suggest the cleavage of the radical ion pair.

Conclusions

A series of molecules each composed of a stable carbanion and carbocation, covalently attached to each other, has been photolysed and studied via picosecond and nanosecond laser techniques. These molecules undergo a sequence of events that begins with absorption of a photon by one of two localized chromophores in each precursor (i.e., the stilbene of TPCP or the aryl portion of the starting carbanion). The constraints of the geometry in the molecules prevent overlap of the π-systems, a result confirmed by the absence of any EDA bands in the UV-visible spectrum and from the fluorescence data. The singlet excited states initiate an electron-transfer event at rates that were too fast to measure under the conditions employed. In other words, the radical ions were observed within the shortest measurement time scale (< ca. 25 ps). The radical ion pairs have two possible alternatives: (1) back electron transfer to form the triplet of the triphenylcyclopropenyl part and (2) bond fragmentation of the central bond (i.e., the one connecting the carbanion to the carbocation). Apparently, the presence of ions from the latter cleavage depends on the relative rates of the two processes. The ions are only observed in those cases where the bond breakage can compete with the back electron transfer. The fragmentation of the radical ion pair can, in principle, give either the ion or radical pair. For the examples in this study, the ions are favored thermodynamically over the radicals, a result that can be predicted (or confirmed) from the redox properties of the ions (i.e., available from electrochemical data). We suggest that the intramolecular radical ion pair is both a novel and a general method for fragmentation of carbon-carbon bonds. We are exploring other systems in which the fragmentation process is greatly enhanced and in which neutral radicals are the ultimate products.

Acknowledgment. We acknowledge the support of the NSF (KSP and EDO) and the Gas Research Institute (EMA and KEM). We are thankful to Steve Angel (Colorado) for measuring picosecond decay kinetics and for discussions concerning kinetic schemes, to Ed Hilinski (Florida State) for suggestions concerning solvent effects on electron-transfer reactions and stilbene cyclization, to T. J. Meyer (North Carolina) for the use of the nanosecond apparatus, and to Earl Danielson and Wayne Jones (UNC) for comments concerning its operation. N.J.P. acknowledges the University of Arkansas and the Department of Chemistry & Biochemistry for a sabbatical leave and Boulder Memorial Hospital for making its completion a possibility.

(42) At 25 °C, 2 mM TPCP-NMN in acetonitrile that contains 40 mM $TPCP^+BF_4^-$ will produce 6.5 μM NMN^- (K_{hetero} = 1.35 × 10^{-4}; ref 1c). At the earliest times recorded in Figure 8, the OD change of 0.05 for NMN^- accounts for an additional 1.7 μM NMN^- (molar absorptivity 3.01 × 10^{-4}; ref 1c). An apparent new K can be determined (from [$TPCP^+$] = 40 mM, [NMN^-] = 8.2 μM, and [TPCP-NMN] = 1.99 mM] and is found to be K_{app} = 1.65 × 10^{-4}. For this to be true under thermal conditions, the new temperature should be 89 °C, representing a rise of 64 °C. If we assume an irradiated volume 1 cm long and 0.5 cm in diameter (ca. 63 μL or 1.2 μmol of acetonitrile), a laser pulse of 20 mJ (20% of the maximum possible output at 355 nm, amplifier at 50% and oscillator at 50%), and a heat capacity of 0.7 cal/mol deg, we predict a temperature jump of ca. 6 °C if all of the laser power becomes heat!

Rare α-Alkyl Isomers of Cobalamins: Synthesis, Characterization, and Properties of Two Diastereomers of the α-Alkylcobalamin, α-(2-Oxo-1,3-dioxolan-4-yl)cobalamin

Yun W. Alelyunas,[†] Paul E. Fleming,[†] Richard G. Finke,*[,†] Thomas G. Pagano,[‡] and Luigi G. Marzilli[‡]

Contribution from the Department of Chemistry, University of Oregon, Eugene, Oregon 97403, and Department of Chemistry, Emory University, Atlanta, Georgia 30322.
Received September 10, 1990

Abstract: The synthesis, characterization, 2-D NMR (HOHAHA, NOESY, HMQC, and HMBC spectroscopies), and reactivities of a new α-alkylcobalamin are described (an α-alkylcobalamin has the axial alkyl group attached to the cobalt from the "bottom" or α face of the corrin ring). The α-alkylcobalamin, α-(2-oxo-1,3-dioxolan-4-yl)cobalamin (**1**), is the first example of an α-alkylcobalamin with a secondary alkyl group and the first case with a chiral alkyl group (i.e., where α-alkylcobalamin diastereomers are produced). It is also the first α-alkylcobalamin completely characterized (HPLC, UV-visible, IR, FAB-MS, and 1- and 2-D NMR methods). Anaerobic photolysis converts **1** to its β isomer, β-(2-oxo-1,3-dioxolan-4-yl)cobalamin (**2**), where the alkyl group is now attached to the cobalt from the usual, β or "top" side of the corrin. Physical properties previously unavailable for any α-alkylcobalamin were measured for **1**, notably the β-side axial base binding constants [for 1-methylimidazole, pyridine, (±)-histidine, and 1,5,6-trimethylbenzimidazole], and the thermal stability of the individual diastereomers of **1**. Possible mechanisms for, and the factors controlling, the formation of α- and β-alkylcobalamins are presented and discussed.

Introduction

The two outstanding examples of a β-alkylcobalamin are β-(5′-deoxyadenosyl)cobalamin (coenzyme B_{12}) and β-methylcobalamin, the β prefix indicating (as usual) that the alkyl group attached to cobalt is on the "upper" face of the structure as shown in Figure 1A for β-methylcobalamin. α-Alkylcobalamins, on the other hand (Figure 1B), are relatively rare and thus little studied; established examples are limited to α-cyanocobalamin,[1-3] α-me-

[†] University of Oregon.
[‡] Emory University.

(1) Work by Friedrich and co-workers provided the discovery and pioneering studies of α-alkylcorrins.[4-7,8b]

0002-7863/91/1513-3781$02.50/0